where x_p is the abscissa of the point P as shown in Fig. 1*a*. The point P is defined as the intersection of the x-axis and the depletion boundary curve under overall gate-induced space-charge neutrality conditions (concept defined in Reference 2). The last approximation is based on two-dimensional numerical analysis performed by means of MINIMOS.

Using the above approximations one can replace all integrals in eqn. 3 by their explicit solutions. This results in a closed-form analytical expression for the potential distribution under the centre of the gate, which is of particular interest in MOS transistor modelling.

Now the values of x_p and $\Psi(0, 0)$ in eqn. 4 remain to be determined, which may be done as follows. After Dang,[3] the junction depletion-layer boundary is assumed to take the form of an ellipse with the centre at the gate end and with diameters $2(w_L + 0{\cdot}7)$ and $2(w_T + x_j)$. Quantities w_L and w_T are shown in Fig. 1*a* and denote lateral and transversal thicknesses of the substrate depletion layer, respectively, under the overall gate-induced space-charge neutrality conditions. Then x_p may be found by simple geometrical transformations as

$$x_p = (x_j + w_T)\sqrt{\{1 - [0{\cdot}7x_j/(w_L + 0{\cdot}7x_j)]^2\}} \tag{5}$$

where x_j is the junction depth.

The value of $\Psi(0, 0)$ is assumed to be

$$\Psi(0, 0) = V_0 + V_S - \frac{kT}{q} \ln [N(0)/N_B] \tag{6}$$

where N_B is the bulk doping concentration, V_S is the applied source voltage and V_0 is the so-called offset voltage defined by Chawla and Gummel.[4]

The work of Chawla and Gummel is based on the approximation of the real junction doping profile by the exponential-constant one and introduces quantities $V_0 = V_g + V_c$ termed as offset voltage, gradient voltage and correction factor, respectively. For simplicity the V_c value, through this study, is taken to be equal to 150 mV instead of a complex expression proposed by Chawla and Gummel. At the end the values of V_g, w_L and w_T are calculated directly by use of appropriate expressions from Reference 4.

As an example of its validity the theory presented in this letter was used for threshold voltage calculation of a typical H-MOS transistor with a strongly nonuniform doping profile shown in Fig. 2. For this purpose the theory was accompanied by the well known relation

$$V_G = V_{FB} + V_S + \Psi\left(0, \frac{L}{2}\right) + \frac{\varepsilon_{Si}}{\varepsilon_{ox}} T_{ox} E_x\left(0, \frac{L}{2}\right) \tag{7}$$

where V_G is the gate voltage, V_{FB} is the flat-band voltage, T_{ox} is the oxide thickness, ε_{Si}, ε_{ox} are the permittivities of silicon and oxide, respectively, and $E_x(0, L/2)$ is the transversal electric field at the semiconductor surface. Afterwards, the following procedure described by Doucet and Van de Wiele[5] was applied. The left-hand side of eqn. 3 rewritten for $x = 0$ was replaced by the surface potential Ψ_c related to the onset of strong inversion (any well known criterion can be used there) and the resulting equation was solved for w. Next, eqn. 3 with this w was differentiated to calculate the transversal surface field $E_x(0, L/2)$ value. Finally the values of $\Psi(0, L/2) = \Psi_c$ and $E_x(0, L/2)$ after substitution into eqn. 7 resulted in the threshold voltage value V_T.

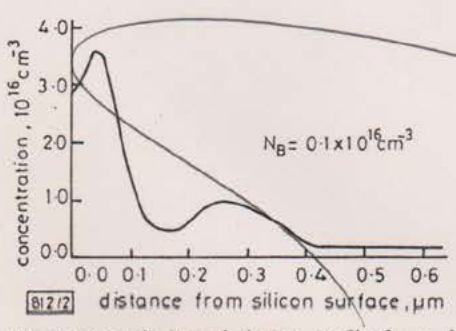

Fig. 2 *Typical channel doping profile for a double boron-implanted H-MOS transistor*

In Fig. 3 some typical results, i.e. $(V_T - V_S)$ dependence on L for various V_S, obtained according to our theory are compared with results of exact two-dimensional numerical calculations

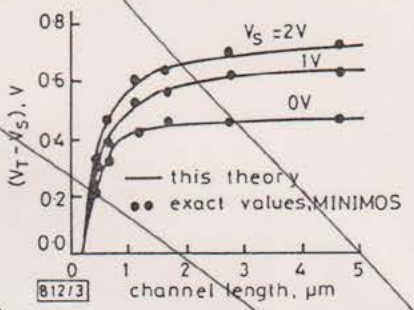

Fig. 3 $(V_T - V_S)$ *against effective channel length L with varying* V_S
Doping profile as shown in Fig. 2
$U_{DS} = 0{\cdot}01$ V; $x_j = 0{\cdot}25$ μm; $T_{ox} = 350$ Å; gate = poli-Si

made by use of MINIMOS, showing excellent agreement in a wide range of L values.

In conclusion, a new effective theory suitable for VLSI MOSFET modelling was presented. This theory allows accurate prediction of the potential distribution in the short-channel case being free of any doping profile averaging but dealing directly with the real profile, which significantly exceeds the insight offered by other theories.

Acknowledgment: The author wishes to express his thanks to Dr. W. Marciniak for helpful discussions and guidance throughout this study, and to Dr. S. Selberherr for providing the MINIMOS program.

T. SKOTNICKI

Institute of Electron Technology, CEMI
Al. Lotników 32/46, 02-668 Warsaw, Poland

31st May 1983

References

1 SELBERHERR, S., SCHÜTZ, A., and PÖTZL, H. W.: 'MINIMOS—A two-dimensional MOS transistor analyzer', *IEEE Trans.*, 1980, **ED-27**, pp. 1540–1550
2 TROUTMAN, R. R.: 'Ion-implanted threshold tailoring for insulated gate field-effect transistors', *ibid.*, 1977, **ED-24**, pp. 182–192
3 DANG, L.: 'A simple current model for short-channel IGFET and its application to circuit simulation', *ibid.*, 1979, **ED-26**, pp. 436–445
4 CHAWLA, B. R., and GUMMEL, H. K.: 'Transition region capacitance of diffused *p-n* junctions', *ibid.*, 1971, **ED-18**, pp. 178–195
5 DOUCET, G., and VAN DE WIELE, F.: 'Threshold voltage of non-uniformly doped MOS structures', *Solid-State Electron.*, 1973, **16**, pp. 417–423

THEORY OF SPONTANEOUS EMISSION IN GAIN-GUIDED LASER AMPLIFIERS

Indexing terms: Lasers and applications, Spontaneous emission

We give an argument suggesting that spontaneous emission in gain-guided laser amplifiers is enhanced by a factor much smaller than the K-factor previously calculated. This is because the fundamental mode content of the spontaneous emission field should be calculated in the sense of the Hermitian rather than direct product at the laser output.

In some semiconductor lasers, the optical wave is guided in the plane of the junction (x, z) by the medium gain rather than by any increase in the real part of the refractive index. Gain-guided modes have a field intensity that falls off exponentially away from the stripe region, but, unlike ordinary modes, they have curved diverging wavefronts. The fundamental modal field $\psi_0(x)$, where x denotes the transverse co-ordinate, is therefore a complex function of x. Petermann[1] has shown that the spontaneous emission power 'in the mode' is enhanced by

a factor $K \gg 1$ in gain-guided lasers with inverted profiles compared to index-guided lasers. Most authors (see the last paragraphs in Reference 2) take it for granted that the spontaneous emission power in such laser amplifiers in the output mode is enhanced by that factor K. The expression 'in the mode', however, is quite ambiguous. The field $\psi(x)$ just outside the laser amplifier may indeed be expressed as the sum of a field in the fundamental mode $\psi_0(x)$ plus something else according to either

$$\psi(x) = \psi_0(x) + \psi'(x) \qquad \int_{-\infty}^{+\infty} \psi_0 \psi' \, dx = 0 \tag{1a}$$

or

$$\psi(x) = \alpha\psi_0(x) + \psi''(x) \qquad \int_{-\infty}^{+\infty} \psi_0^* \psi'' \, dx = 0 \tag{1b}$$

where the star denotes complex conjugate value. The modulus of the constant α may be very different from unity. The point made in this letter is that mode filters (nondegenerate lossless optical cavities, heterodyne optical receivers, beats between signal and spontaneous emission[3] ...) measure the power in $\alpha\psi_0$ according to eqn. 1*b* and not the power in ψ_0 according to eqn. 1*a*. It follows from this observation that spontaneous emission in the mode (as we have just defined it) from the output end of a laser amplifier is not enhanced at all. If there is a strong mode-filtering action in the gain-guided laser favouring the fundamental mode, then the spontaneous emission originating from the input end of the laser is mainly in the ψ_0 mode at the output end, and for that part of the spontaneous emission Petermann's K-factor does apply.

It is therefore important to determine whether gain-guided lasers actually provide strong filtering of higher-order modes. We will show that in general they do not, because laser amplifiers have rather wide stripes.[2]

In order to have analytical solutions, let us assume, as in Reference 1, that the complex index of refraction follows a square-law:

$$k(x) = k_0[1 + \Delta(x/d)^2] - i\tfrac{1}{2}N_0[1 - (x/d)^2] \tag{2}$$

where $k = (\omega/c)n$. The parameter $2d$ is roughly the stripe width. Antiguiding increases with the relative index change $\Delta > 0$ at the stripe edge. The imaginary term in k is proportional to the density of atoms or electron-hole pairs responsible for both stimulated and spontaneous emission. The solution for the modal fields and the gains in the medium described by eqn. 2 is well known (see, for example, Reference 4) and need not be repeated here. We will in the following assume that antiguiding is very strong because this is the most interesting case.

We shall impose the condition that the $\psi_0(x)$ field intensity is negligible in the region where the medium has loss instead of gain. Otherwise the ratio $P_{sp}/(G-1)$, where G denotes the power gain, would be enhanced by a factor gain/(gain-loss) quite aside from the effect of wavefront curvature that we are studying. This condition may be written, from Appendix 1, as

$$N_0 d \gg \sqrt{(2\Delta)} \tag{3}$$

The gain of mode m is (see Reference 4; eqn. 8)

$$\gamma_m = \tfrac{1}{2}N_0 - (m + \tfrac{1}{2})\sqrt{(2\Delta)}/d \tag{4}$$

A more general result is given in Appendix 2. Under the condition in eqn. 3 the net gain of the amplifier is approximately $1/2N_0 L$ if L denotes the laser length. For example, for a net gain of 10 dB, $N_0 L = 2{\cdot}3$ and the ratio of the field intensities of two modes at the laser output, assuming equal excitation:

$$|\psi_1/\psi_0| \simeq \exp[(\gamma_1 - \gamma_0)L] = \exp(-2{\cdot}3\sqrt{(2\Delta)/N_0 d}) \tag{5}$$

is close to unity according to eqn. 3. Thus mode filtering is weak for practical laser gains when the calculated K-factor is large, and consequently the effective spontaneous emission enhancement factor of gain-guided laser amplifiers 'in the mode' may be much smaller than K. In order to get precise numbers, rather involved calculations are needed that will be reported elsewhere.

The author expresses his thanks to J. C. Simon for his comments on an earlier version of this letter.

J. ARNAUD

Equipe de Microoptoelectronique de Montpellier
USTL, Pl. E. Bataillon
34060 Montpellier, France

2nd June 1983

References

1 PETERMANN, K.: 'Calculated spontaneous emission factor for double-heterojunction injection lasers with gain-induced astigmatism', *IEEE J. Quantum Electron.*, 1979, **QE-15**, pp. 566–570
2 MARCUSE, D.: 'Computer model of an injection laser amplifier', *ibid.*, 1983, **QE-19**, pp. 63–73
3 ARNAUD, J.: 'Enhancement of optical receiver sensitivity by amplification of the carrier', *ibid.*, 1968, **QE-4**, pp. 893–899
4 ARNAUD, J.: 'Beam and fiber optics' (Academic Press, NY, USA, 1976)

Appendix 1: The expression of the modal field:[4]

$$\psi_0(x) = \exp(-\tfrac{1}{2}k_0 \Omega x^2) \tag{6}$$

is applicable to square-law media with gain according to eqn. 2 if we set ($N_0 \ll k_0$):

$$\Omega^2 = -2\Delta/d^2 - iN_0/k_0 d^2 \tag{7}$$

i.e., approximately for strong antiguiding,

$$\Omega \simeq -i\sqrt{(2\Delta)}/d + N_0/(2\sqrt{(2\Delta)}k_0 d) \tag{8}$$

The fundamental mode halfwidth ξ_0 is therefore given from eqns. 6 and 8 by

$$d^2/\xi_0^2 = N_0 d/2\sqrt{(2\Delta)} \tag{9}$$

In the main text we explain why, for reasons of consistency, we must assume that this quantity is much larger than unity. The conditions set up in this letter are consistent provided the Fresnel number $d^2/\lambda L \gg 1$. This is the case for rather wide-stripe short laser amplifiers. Note that the K-factor defined in eqn. 15:

$$K = [1 + (4\Delta k_0/N_0)^2]^{1/2} \tag{10}$$

does not depend on the stripe width d in our large Δ square-law model.

Appendix 2: It has been shown in Reference 1 that the spontaneous emission power P_{sp} is enhanced in gain-guided lasers by a factor $K > 1$. We show here that the important parameter $P_{sp}/(G-1)$ is indeed proportional to K if mode filtering is very strong.

For a mode $\exp[i(\beta z - \omega t)]$ the wave equation for the optical field $\psi(x)$ is[4]

$$\beta\psi = k(x)\psi + \tfrac{1}{2}k_0^{-1} \, \partial^2\psi/\partial x^2 \tag{11}$$

If we set $\beta = \beta_0 - i\gamma$ and $k(x) = k_r(x) - ig(x)$, multiply both sides of eqn. 11 by ψ^*, integrate from $x = -\infty$ to $+\infty$, neglect in the second term the imaginary part of $k_0 = k(0)$ (a permissible approximation), and note that $\psi \to 0$ as x approaches infinity, we get the power conservation law

$$\gamma = \int_{-\infty}^{+\infty} g(x)|\psi_0|^2 \, dx \Big/ \int_{-\infty}^{+\infty} |\psi_0|^2 \, dx \tag{12a}$$

where $|\psi|^2 = \psi\psi^*$. For a slice comprised between z and $z + dz$, the power gain G is

$$G - 1 = 2\gamma \, dz \tag{12b}$$

Now, the term g responsible for stimulated emission in eqn. 12 is also responsible for spontaneous emission. We can view $\eta g(x') \, \delta(x - x')$, where $\eta = (2h\nu \, dz)^{1/2}$ and $\delta(.)$ is the Dirac function, as the field emitted spontaneously at x'. This field can be expanded in the modal fields $\psi_m(x)$ according to

$$\eta g(x') \, \delta(x - x') = \sum_m \eta g(x')\psi_m(x')\psi_m(x) \Big/ \int_{-\infty}^{+\infty} \psi_m^2(x) \, dx \tag{13}$$

where we have used the well known orthogonality condition for modes in waveguides with gain or loss. The spontaneous emission power in the fundamental mode is obtained by integrating over x the modulus square of the term properional to $\psi_0(x)$ in eqn. 13 and integrating that power from $x' = -\infty$ to $+\infty$. We readily obtain for that slice comprised between z and $z + dz$

$$P_{sp} = h\nu(G - 1)K \tag{14}$$

where $G - 1 = 2\gamma \, dz$, γ is given in eqn. 12*a* and

$$K = \left(\int |\psi_0|^2 \, dx \Big/ \left| \int \psi_0^2 \, dx \right| \right)^2 \tag{15}$$

is Petermann's K-factor.

TWO-PARAMETER EMPIRICAL MODEL FOR RAINFALL RATE DISTRIBUTION

Indexing terms: Radiowave propagation, Rain

In a previous paper we suggested a three-parameter model providing a good fit for rate distribution. Moreover, this model approximates a log-normal distribution at low rates and a gamma distribution at high rates. In the letter we reduced the number of parameters to two by setting the third one constant. This modified model appears to give good agreement with the experimental data gathered in various locations around the world.

Log-normal and gamma distributions can provide rather good approximations for low and high rainfall rates, respectively, but, as is well known, none of these models can accurately account for rainfall rate cumulative distribution.[1]

Recently, from rainfall measurements carried in Brazzaville (Congo),[2] the author suggested[3,4] an empirical but theoretical sound model[5] providing a better fit for a rain-rate cumulative distribution. This model involves a single function for the whole range of relevant values, approximating the gamma distribution at high rain rates and the log-normal distribution at the low rates.

According to this model, the probability that a rainfall rate R exceeds r is given by

$$P(R \geq r) = a \frac{e^{-ur}}{r^b}, \quad r \geq 2 \text{ mm/h} \tag{1}$$

where a, b and u are parameters depending on the integration time of the rain gauge and on the climate.

Then, the distribution function of the rain rates r and its probability density are given by

$$F(r) = P(R \leq r) = 1 - P(R \geq r) \tag{2}$$

$$f(r) = \frac{dF(r)}{dr} \tag{3}$$

From these equations it has been shown[4] that: $0 < a < 1$; $0 < u < 1$; $b > 0$.

In previous papers we considered the possibility of setting constant one out of these parameters for all climatic areas, in order to reduce the number of parameters. This is achieved in this letter.

The comparison of our empirical model with the gamma and log-normal distributions was already discussed[4-6] and here we will merely give some examples of our empirical law approximations with one fixed parameter.

The value of u which leads to the best fit of the various hydrometeorological zones is

$$u = 2{\cdot}5 \times 10^{-2}$$

a and b being functions of the climate and the integration time.

Figs. 1 and 2 show rainfall rate data from various countries[7,8] fitted by our model.

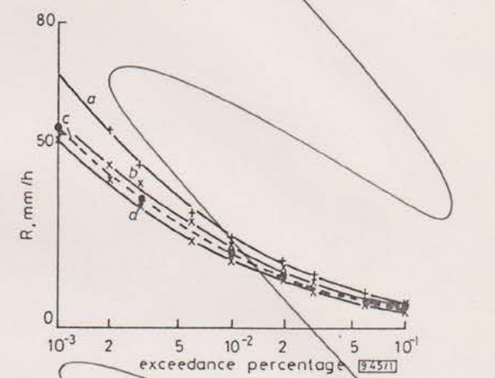

Fig. 1 *Rain-rate statistics*

a Stockholm (Sweden)	1976–77	$a = 0{\cdot}012$;	$b = 1{\cdot}29$
b Darmstadt (W. Germany)	1976	$a = 0{\cdot}014$;	$b = 1{\cdot}45$
c Kjeller (Norway)	1975–76	$a = 0{\cdot}012$;	$b = 1{\cdot}45$
d Mendlesham (UK)	1973–75	$a = 0{\cdot}01$;	$b = 1{\cdot}44$

Integration time = 1 min

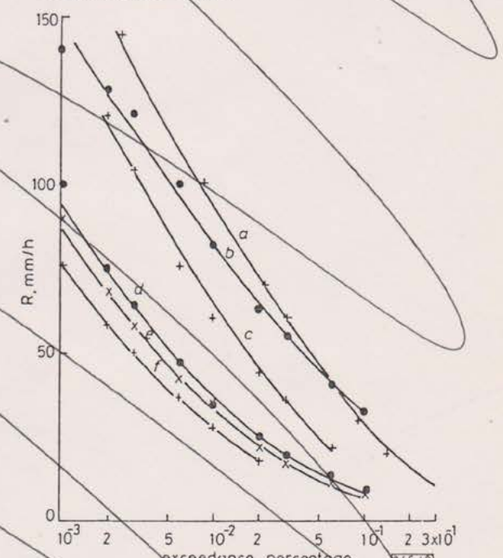

Fig. 2 *Rain-rate statistics*

a Brazzaville (Congo)	1980–81	$a = 1{\cdot}44 \times 10^{-2}$;	$b = 0{\cdot}57$

Integration time = 6 min

b Calcutta (India)	1979–80	$a = 0{\cdot}1$;	$b = 1{\cdot}1$
c Holmdel (USA)	1968–69	$a = 6 \times 10^{-3}$;	$b = 0{\cdot}59$
d Fucino (Italy)	1975–77	$a = 0{\cdot}011$;	$b = 1{\cdot}03$
e Paris (France)	1972–77	$a = 0{\cdot}01$;	$b = 1{\cdot}07$
f Louvain (Belgium) La Neuve	1970–75	$a = 7{\cdot}56 \times 10^{-3}$;	$b = 1{\cdot}09$

Integration time = 1 min

In its report 563-2[3] (see Table 1 and Figs. 11 to 13), CCIR gives rain hydrometeorological zone intensities across the world.